

Salt template zirconia reinforcing particles as possible reinforcement for PMMA matrix composite

AA Elmadani¹, N Tomić², I Radović³, MM Vuksanović³ ,
D Stojanović¹, R Jančić Heinemann¹ and V Radojević¹

Abstract

To obtain flakes like zirconia particles at relatively low temperature, the synthesis method for producing zirconia particles on the surface of salt particles that serve as a template is examined. The produced particles are incorporated as reinforcement in the poly(methyl methacrylate) matrix to obtain a composite material. The particles were characterized by the X-ray diffraction, Fourier-transform infrared spectroscopy, and image analysis. The morphology of the particles and composites was examined using a field emission scanning electron microscope. Composites prepared with synthesized particles were compared to those containing commercial zirconia particles to estimate the possibility of use of synthesized particles as reinforcement. The influence of the 1 wt% of zirconia particles in composite material on the mechanical properties was studied using microhardness measurements and dynamic mechanical analysis. The results obtained show that the addition of 1 wt% of zirconia particles increases the mechanical properties of the composite relative to the pure polymer matrix.

Keywords

zirconia, composites, sintering, mechanical properties, microhardness

Introduction

Zirconia is one of the important ceramics, which, due to its high mechanical strength and fracture toughness, is widely used. The biocompatibility of zirconia enables its use as a biomaterial. Electrical, mechanical, optical, and thermal properties of zirconia are resulting in a wide application, such as structural materials, thermal barrier coating, solid oxide fuel cell electrolytes, and semiconductor materials. It can also be used as a catalyst in various reactions, such as isomerization of alkanes, dehydration of an alcohol, and nitrogen oxide decomposition.¹ Due to its good mechanical properties and biocompatibility, the zirconia is increasingly used as an implant in the field of dental medicine.² Zirconia has been synthesized by different methods, such as combustion synthesis, ion exchange, solid-state reaction, sol-gel synthesis, glycothermal processing, Pechini method, and a wet chemical method.^{3,4}

Zirconium dioxide (ZrO₂) is a ceramic material that has become attractive due to its mechanical, thermal, and chemical properties and is becoming also very important

as reinforcement in polymer matrix composites.⁵ It may be used in transparent optical devices,⁶ electrochemical capacitor electrodes, oxygen sensors,⁷ fuel cells⁸ as catalyst support⁹ and as a biomaterial. ZrO₂ has several crystal structures and the mechanical properties are dependent on the dominant crystal structure of the powder. The crystallinity of zirconia is defined as monoclinic at room temperature; at higher temperatures, it is tetragonal and cubic.

¹ Faculty of Technology and Metallurgy, University of Belgrade, Karnegijeva, Belgrade, Serbia

² Innovation Center of Faculty of Technology and Metallurgy, Karnegijeva, Belgrade, Serbia

³ Institute of Nuclear Science "Vinca" Belgrade, University of Belgrade, Belgrade, Serbia

Date received: 15 November 2018; accepted: 29 August 2019

Corresponding author:

MM Vuksanović, Institute of Nuclear Science "Vinca", University of Belgrade, P.O. Box 522, 11001 Belgrade, Serbia.

Email: mdimitrijevic@tmf.bg.ac.rs



Creative Commons Non Commercial CC BY-NC: This article is distributed under the terms of the Creative Commons

Attribution-NonCommercial 4.0 License (<http://www.creativecommons.org/licenses/by-nc/4.0/>) which permits non-commercial use, reproduction and distribution of the work without further permission provided the original work is attributed as specified on the SAGE and Open Access pages (<https://us.sagepub.com/en-us/nam/open-access-at-sage>).

Cubic and orthorhombic phases were detected in nano-sized zirconia.¹⁰

Nanocomposites are increasingly studied in recent years especially those that are made of the polymer matrix and inorganic filler due to the ease of preparation, good mechanical and chemical properties, and ease of preparation and handling. Such composites combine the properties of inorganic materials (such as rigidity and thermal stability) with the properties of organic materials (e.g., flexibility, dielectricity, ductility, and processability).¹¹

Poly(methyl methacrylate) (PMMA) is an excellent material, which, due to its properties, has a wide application in optical fibers, optical discs, and lenses. PMMA, in combination, with inorganic materials, such as SiO₂, TiO₂, or zirconium oxide (ZrO₂), makes hybrid materials having high strength and thermal stability.^{12,13}

Composites enable adjusting the properties by choosing the adequate matrix as well as the reinforcement. As a matrix material, polymers are often considered for their ease of handling and good forming properties. The morphology and the crystal structure of the reinforcement have a decisive role for the composite properties.¹⁴ The aim of this article was the preparation of ZrO₂ particles from the soluble zirconium salt deposited on a template like a salt crystal and the study of the influence of those preparation conditions on the properties of the obtained particles viewed as the reinforcement in the composite material. Mechanical properties of the prepared composite material were studied using the microhardness and dimethyl acrylate (DMA). The characterization of obtained particles was done by X-ray diffraction (XRD), Fourier-transform infrared (FTIR) spectroscopy, and image analysis.

Experimental procedure

Materials

For composite preparation, acrylic resin (commercially available as Biokril, Galenika AD, Serbia) was used as a polymer matrix. It was a two-component starting kit—powder and liquid. The powder consisted of PMMA polymer and initiator benzoyl peroxide. The liquid part contained MMA monomer and a small amount of ethylene glycol dimethyl acrylate used as a chemical activator. Biokril powder was characterized as follows^{14,15}: $M_n = 1.27 \times 10^5$ g Mol⁻¹, $M_w = 3.82 \times 10^5$ g Mol⁻¹, with a polydispersity, PI = 3.01, and content of MMA was 4.3 wt%. For the preparation of Zirconia by salt method, starting materials were ZrCl₂O · xH₂O powder (ThermoFisher (Kandel), Germany), ethanol, and NaCl (Lach-Ner, s.r.o., Czech Republic). For comparison, the commercial micro-sized Zirconia (ZrO₂ M), Sigma Aldrich, was used as inorganic reinforcement.

Preparation of particles

For the salt template method, a quantity of 125 mg of ZrCl₂O · xH₂O was dispersed in 30 ml of absolute ethanol with vigorous stirring for 1 h. After that, the solution was mixed with 100 g of NaCl fine crystalline powder and dried at 65°C with stirring during 24 h. The mixture was heated with a ramp rate of 2°C min⁻¹ under an Ar atmosphere and annealed at 280°C for 2 h. Further treatment included annealing at 750°C for 5 h with a ramp rate of 1°C min⁻¹ under a mixture of NH₃ (10%) and Ar. The product was washed by deionized water to remove salt and centrifuged at 3000 r min⁻¹ for 30 min. The sample was vacuum-filtrated and collected for further treatment. Finally, the powder was annealed at 1150°C during 5 h in Air atmosphere. The obtained particles were marked as ZrO₂ N.

Preparation of composites

To obtain essential information about the as-synthesized particles, the composite samples were prepared. For the preparation of pure acrylic resin (PMMA), the producer instructions were followed: liquid has been poured in a glass container and the powder was added in a ratio of powder to liquid 2:1 in weight, with continuous mixing performed for 40–45 s. The aluminum mold was filled with solution, closed, and then heated to 70°C for 1 h, followed by the increase of temperature up to 100°C for 30 min, to reduce the content of the residual monomer.¹⁴ For the processing of composites, the same procedure was used with synthesized and commercial particles. Particles were dispersed in the liquid part of starting kit in an ultrasonic bath for 1 h. The mixture was added to the (PMMA) powder and placed in the mold. The thermal treatment was the same as for the pure resin. The particle content in both composites was 1 wt%. In our previous research, composites with 1, 3, and 5 wt% of pure zirconia and acryl resin were processed, and the best impact and overall mechanical behavior were achieved with 1 wt% of reinforcements.^{11,15} In accordance with these findings, this research introduces a comparison of composites with 1 wt% of synthesized and commercial particles. The composites with synthesized and commercial zirconia particles are denoted as PMMA/ZrO₂ N and PMMA/ZrO₂ M, respectively.

Characterization methods

The morphologies of the ZrO₂ particles and composites were examined using a field emission scanning electron microscope (FE-SEM), TESCAN MIRA3 XMU, operated at 20 kV. Morphological parameters of particles were determined using the image analysis tools (Image-Pro Plus 6.0, Media Cybernetics Inc., Cambridge, UK).¹⁶

X-ray powder diffraction (XRPD) patterns were recorded with an Ital Structure APD2000 X-ray diffractometer in a Bragg–Brentano geometry using CuKα

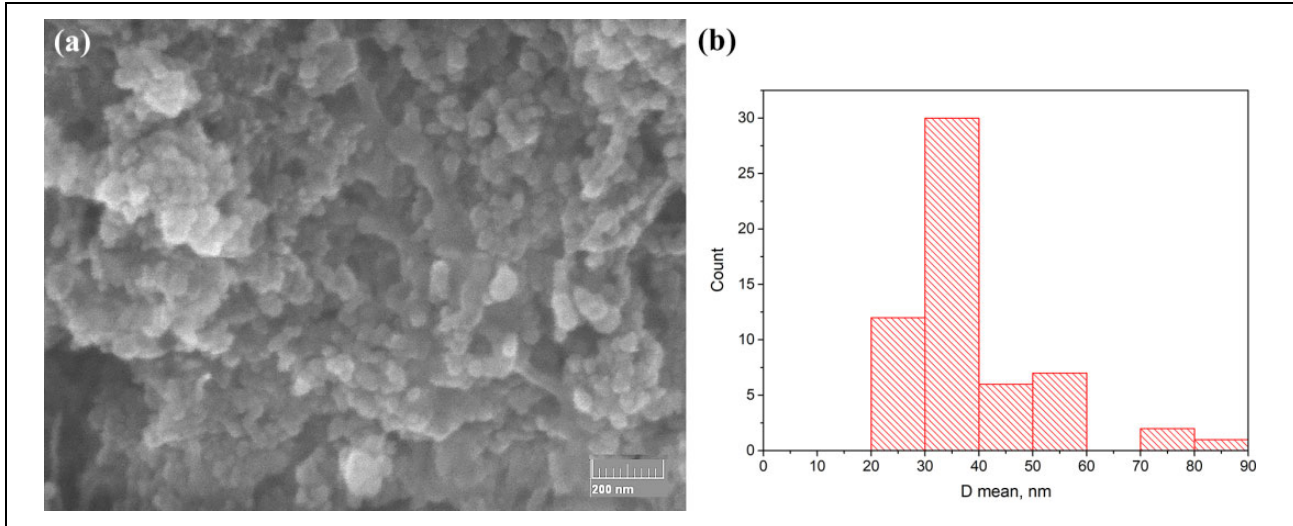


Figure 1. (a) The SEM micrographs of ZrO_2 particles and (b) diameter distribution. SEM: scanning electron microscope.

radiation ($\lambda = 1.5418 \text{ \AA}$) and step-scan mode (range: $20\text{--}80^\circ 2\theta$, step-time: 0.5 s, step-width: 0.02°).

The structural analysis of ZrO_2 particles and composites was performed by single-beam FTIR using a Nicolet 6700 spectrometer (Thermo Scientific) in the attenuated total reflectance (ATR) mode using a single bounce $45^\circ F$ Golden Gate ATR accessory with a diamond crystal and an electronically cooled DTGS detector. The spectra were the co-addition of 64 scans at 4 cm^{-1} spectral resolution and were ATR corrected. The Nicolet 6700 FT-IR spectrometer was equipped with OMNIC software and recorded the spectra in the wavelength range from $2.5 \text{ }\mu\text{m}$ to $20 \text{ }\mu\text{m}$ (i.e. 4000 cm^{-1} to 500 cm^{-1}).

The microhardness of the composite systems was characterized using micro Vickers hardness value (HV) tester Leitz, Kleinhartepreifer DURIMETI using an original quadrangular pyramid diamond indenter with an angle of 136° .¹⁷ To obtain reproducible HV, microhardness of PMMA composites without particles and PMMA composites with ZrO_2 particles was measured applying a load of 500 g for 25 s. For each sample, three indents were performed at room temperature according to ASTM E384-16.¹⁸ Image-Pro Plus program was used to obtain the diagonal lengths from images obtained by the optical microscope, Carl Zeiss—Jena, NU2. The average results of diagonal were taken from the reported measurement for calculation of microhardness using the following equation:

$$VHN = 2 \cos \frac{22^\circ P}{d^2} = \frac{1.8544P}{d^2}$$

where P (kgf) stands for the applied load and d (mm) is the length of the indentation diagonal.¹⁹

The dynamic mechanical analysis was used to examine the performance of the PMMA matrix composite reinforced using ZrO_2 particles. The data obtained from this analysis included the storage modulus (G'), tangent delta

($\tan \delta$), and the glass transition temperature (T_g). The storage modulus reveals the ability of the composite to store elastic energy associated with recoverable elastic deformation. Together with $\tan \delta$, the storage modulus describes the behavior of the composite under stress in a defined temperature range. DMA was performed on a DMA Q800 (TA Instruments) under a nitrogen atmosphere in the single cantilever mode. Storage modulus and loss factor ($\tan \delta$) were determined for rectangular specimens of size $35 \times 13 \times 3 \text{ mm}^3$ at a frequency $\omega = 1 \text{ Hz}$. The temperature range was changed from room temperature to 160°C at a heating rate of 3°C min^{-1} .²⁰

Results and discussion

Microstructure of the particles and composites

The SEM micrographs and diameter distributions of prepared ZrO_2 particles are shown in Figure 1.

The diameter distribution was obtained from the image of the specimen showing a large number of agglomerated particles. Using Image Pro-Plus software, single particles were selected on the image and two diameters of each recognized particle were measured. Based on these measurements, the software recognized formed agglomerates.^{21,22} The obtained result indicates that the obtained particles were fine, having diameters mostly under 100 nm. Several particles that were larger are possibly agglomerates of two separated particles that cannot be distinguished on the image clearly.

The morphology and the distribution of zirconia particles were examined using scanning electron microscopy. The cross-sectional view obtained from the composite fracture surfaces using SEM is shown in Figure 2. The particles were in both cases very fine in diameter and well distributed in the structure. Composites with commercial zirconia particles had small agglomerates, which are arranged in a

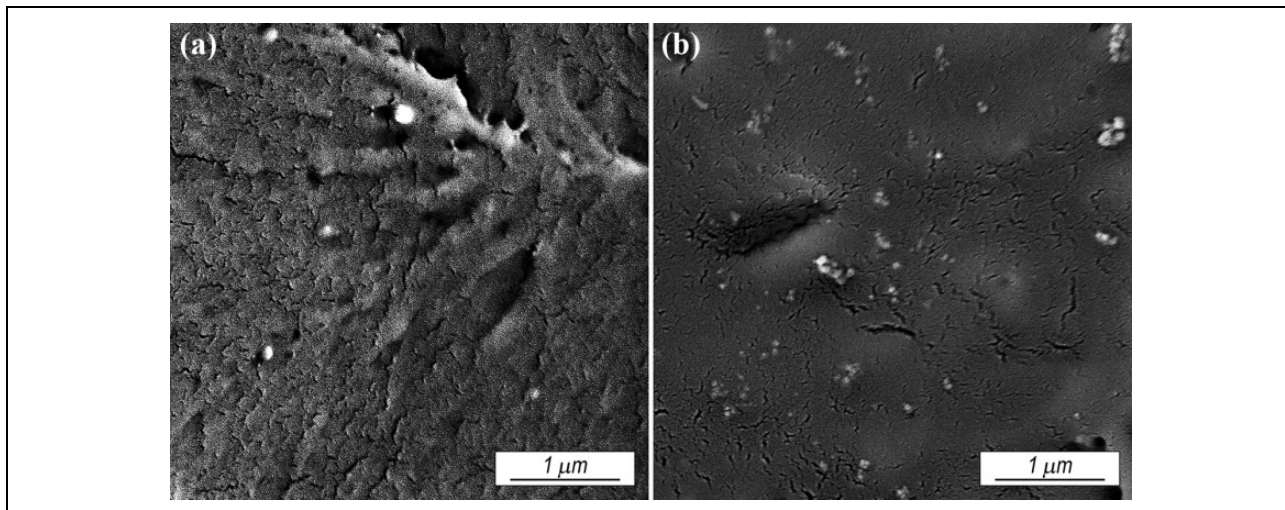


Figure 2. Cross section of the fracture surface of studied composites (a) the composite with synthesized particles and (b) the composite with commercial particles.

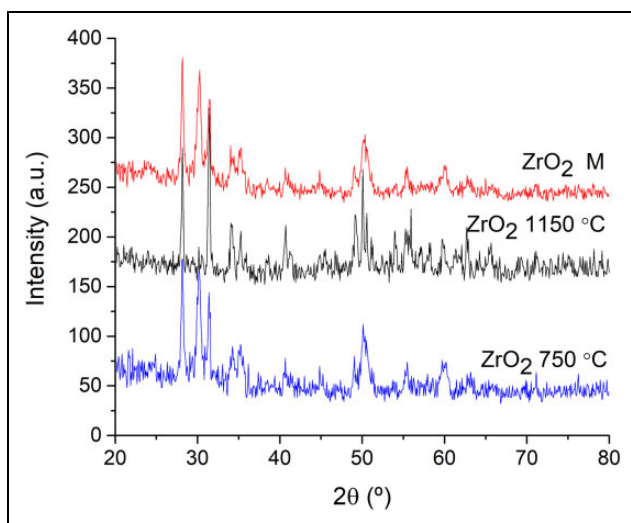


Figure 3. XRD patterns of ZrO_2 M particle and ZrO_2 N particles at 750°C and 1150°C. XRD: X-ray diffraction.

polymeric matrix, leading to reduced mechanical properties compared to composites with synthesized zirconia particles.

XRD analysis of particles crystal structure

XRD is used to identify the crystalline structure (Figure 3). By the XRPD technique, the ZrO_2 phase was confirmed by comparison of the XRD data to the standard card 72698-ICSD and $Zr_7O_{11}N_2$ by card 157959-ICSD. The program PowderCell²³ was used for approximate phase analysis. The mean crystallite size of ZrO_2 and $Zr_7O_{11}N_2$ phase was estimated from the most intensive diffraction peaks by the program PowderCell.

The sample (ZrO_2 N) identified at 750°C in the presence of two phases: m- ZrO_2 and $Zr_7O_{11}N_2$. The approximate

mass ratio of the two phases in the sample is 60:40 = m(ZrO_2):m($Zr_7O_{11}N_2$). Unit cell parameters of m- ZrO_2 phase are $a = 5.1475$, $b = 5.2253$, and $c = 5.3213$. Unit cell parameters of $Zr_7O_{11}N_2$ phase are $a = 9.5973$ and $c = 17.6910$. At 1150°C in the sample identified the mass ratio of the two phases 93:7 = m(ZrO_2):m($Zr_7O_{11}N_2$) particles. In the sample (ZrO_2 M), two polymorphic crystalline phases ZrO_2 were identified: monoclinic m- ZrO_2 and tetragonal t- ZrO_2 . The approximate mass ratio of the two phases in the sample is 64:36 = m- ZrO_2 :t- ZrO_2 . The identification of the m- ZrO_2 phase was performed by comparing the experimental values with the card 72698-ICSD and the t- ZrO_2 phase with the 66781-ICSD card. In the preparation of composites, the powder synthesized at 1150°C was used. The commercial powder was used for the purpose of comparing the mechanical properties that are obtained using those two types of the crystal structure.

Structure characterization via FTIR spectroscopy

The FTIR spectra of obtained particles and composites are shown in Figure 4.

The FTIR spectra of the synthesized zirconia particles, PMMA matrix, and obtained composite are presented (Figure 4). The FTIR spectrum of Figure 4 showed no visible band around 3400 cm^{-1} assigned to the symmetric stretching of OH bonds corresponding to physically adsorbed water on the solid. The band noticed at 584 cm^{-1} can be assigned to Zr-O bond vibrations in monoclinic ZrO_2 .²⁴ The intense vibration noticed at approximately 1100 cm^{-1} may be assigned to the zirconyl bond (Zr=O).²⁵ The weak broadband at 526 cm^{-1} has been reported to be related to crystalline ZrO_2 .²¹

The ethylene C-H stretch bands for PMMA, PMMA/ ZrO_2 , and composites at 2998, 2951, 2924, and 2850 cm^{-1} were sharp²⁶ and in similar positions for both of samples

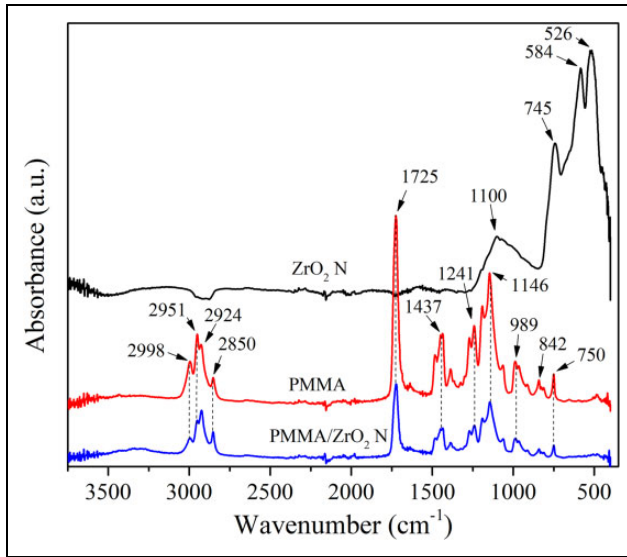


Figure 4. FTIR spectra of ZrO_2 N particles, pure PMMA, and composites with 1 wt% of ZrO_2 N particles. FTIR: Fourier-transform infrared; PMMA: poly(methyl methacrylate).

(Figure 4). The spectra display a typical carbonyl $C=O$ stretch band (approximately 1725 cm^{-1}). Other bands present in the spectrum of PMMA are a doublet of medium intensity in the region of $1500\text{--}1425\text{ cm}^{-1}$, a medium-to-strong band approximately 1146 cm^{-1} , and a medium-intensity band at 750 cm^{-1} .²⁷ Two characteristic peaks at region $1140\text{--}1160\text{ cm}^{-1}$ related to the methyl ester groups of PMMA. One can notice that there is no appearance of new bond vibrations or the change of peak position, suggesting that there was no obvious effect of particle incorporation in the PMMA matrix.

Microhardness of composites and dynamic mechanical analysis

Micrographs of micro Vickers indentation for the outer surface of composites with 1 wt% of ZrO_2 particles are shown in Figure 5.

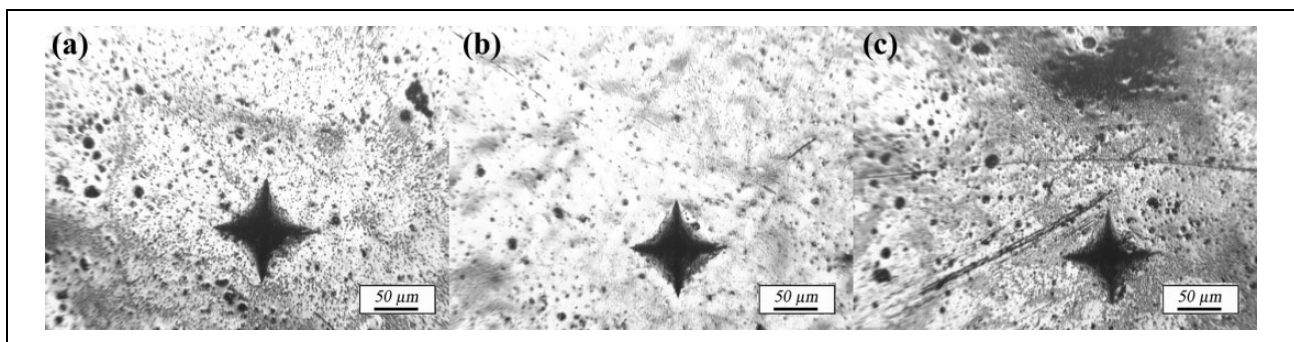


Figure 5. Micrograph of micro Vickers indentation for composites: (a) PMMA, (b) PMMA/ ZrO_2 M, and (c) PMMA/ ZrO_2 N. PMMA: poly(methyl methacrylate).

The obtained values of the microhardness and dynamic mechanical analysis of the composite based on PMMA and with 1 wt% of the different particles are presented in Table 1.

Microhardness of composites with the addition of 1 wt% of the ZrO_2 N particles increases by 23% compared to the pure matrix material while increasing in a composite containing 1 wt% ZrO_2 M particles 17.3%. The properties of zirconia modifications were studied and calculated from the structural crystal parameters showing that the modulus, bulk, shear, and Young are higher for the monoclinic compared to the tetragonal structure.²⁸ The difference between the powders used is essential in the presence of monoclinic crystal modification of zirconia in synthesized particles; they consisted essentially of monoclinic modification, commercial ones had only 60%, and the improvement of hardness is proportional to the quantity of monoclinic structure in the reinforcement.

The addition of ZrO_2 influences the mechanical properties, as observed by DMA analysis (Figure 6). The storage modulus has been measured for the matrix material and the composites, and it was revealed that 1 wt% of synthesized particles ZrO_2 N in the sample slightly improved the storage modulus in the glassy state (G'_{GS}) (around 2%). The commercial particles gave even a larger increase of the storage modulus at low temperatures. The storage modulus in the rubbery state (G'_{RS}) had the largest value for the pure matrix, and the addition of particles decreased the modulus at elevated temperatures. The glass transition temperature remained essentially the same as the particles seem not to build the chemical bond between the matrix and the reinforcement.

On the other hand, synthesized ZrO_2 N particles gave the material a larger value of hardness, as measured by the Vickers method. The hardness is higher, compared to the samples with commercial zirconia particles. This difference in the mechanical behavior of ZrO_2 N and ZrO_2 M could be explained in different crystal structure and content of m- ZrO_2 . In addition, the presence of $Zr_7O_{11}N_2$ in synthesized zirconia leads to different dynamical properties and toughening mechanism.^{29–31}

Table 1. Mechanical properties of PMMA and PMMA composites reinforced with zirconia-based particles.

Samples	HV, GPa	Storage modulus (G'_{GS}), MPa	Storage modulus (G'_{RS}), MPa	$\tan \delta$ peak (T_g), °C
PMMA	0.052 ± 0.001	2189 ± 8	4.08 ± 0.18	133.9 ± 0.3
PMMA/ZrO ₂ N	0.064 ± 0.002	2231 ± 11	3.66 ± 0.45	134.7 ± 0.4
PMMA/ZrO ₂ M	0.061 ± 0.001	2277 ± 17	3.94 ± 0.63	133.9 ± 0.2

PMMA: poly(methyl methacrylate); HV: hardness value.

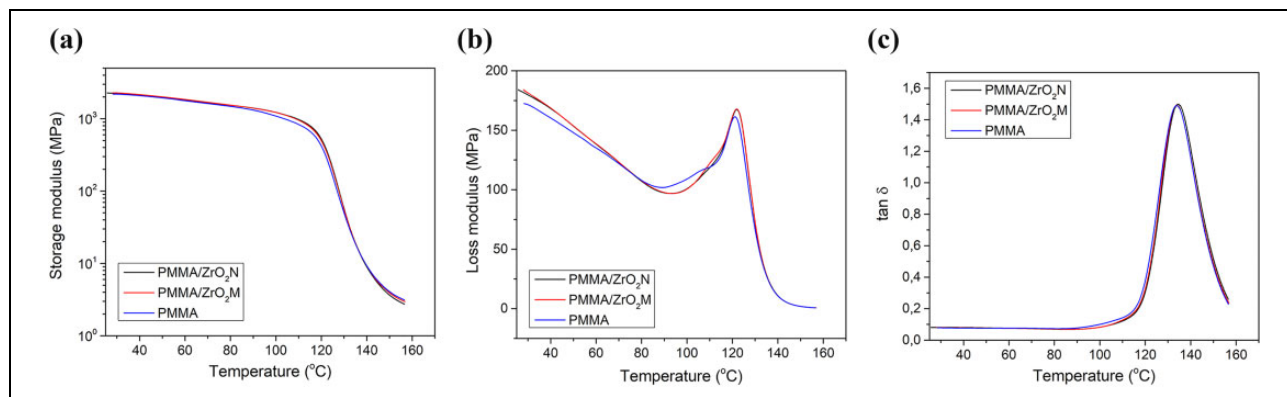


Figure 6. Changes in the storage modulus for the PMMA matrix and composites reinforced with ZrO₂ particles. PMMA: poly(methyl methacrylate).

Conclusion

Zirconia particles were synthesized by the salt template method. The obtained particles had flake-like morphology and fine dimensions. Composites having PMMA as a matrix and synthesized zirconia particles have improved mechanical properties, such as storage modulus and micro-hardness. The results were compared to the composite obtained using commercial zirconia powder. The hardness of the composite with synthesized particles was better compared to the composite processed with commercial zirconia, which can be explained via the crystal structure of reinforcing particles and their content of monoclinic crystal structure. The storage modulus was comparable for both synthesized composites and was superior compared to the pure matrix material in the glassy state. The storage modulus was inferior to the matrix in the rubbery state. The glass transition temperature was not changed and that subjects that the chemical bonding was not established between the particles and the matrix material.

Acknowledgements

The authors wish to acknowledge Galenika enterprise for the cooperation in the discussion of the results and provision of the polymers used in their production.


Declaration of conflicting interests

The author(s) declared no potential conflicts of interest with respect to the research, authorship, and/or publication of this article.

Funding

The author(s) disclosed receipt of the following financial support for the research, authorship, and/or publication of this article: This research has been financed by the Ministry of Education, Science and Technological Development of the Republic of Serbia as a part of the project TR34011.

ORCID iD

MM Vuksanović  <https://orcid.org/0000-0003-1872-195X>

References

- Heshmatpour F and Aghakhanpour RB. Synthesis and characterization of nanocrystalline zirconia powder by simple sol-gel method with glucose and fructose as organic additives. Preparation of zirconia dental crowns via electrophoretic deposition. *Powder Technol* 2011; 205: 193–200.
- Oetzel C and Clase R. Preparation of Zirconia dental crowns via electrophoretic deposition. *J Mater Sci* 2006; 41: 8130–8137.
- Thakare V. Progress in synthesis and applications of Zirconia. *Int J Eng Res Dev* 2012; 5: 25–28.
- Feng G, Jiang W, Liu J., et al. A novel green nonaqueous sol-gel process for preparation of partially stabilized zirconia nanopowder. *Process Appl Ceram* 2017; 11: 220–224.
- Zhu WZ, Lei TC, Zhou Y, et al. Kinetics of isothermal transition from tetragonal to monoclinic phase in ZrO₂ (2 mol% Y₂O₃) ceramic. *Mater Chem Phys* 1996; 44: 67–73.
- Alaniz JE, Perez-Gutierrez FG, Aguilar G, et al. Optical properties of transparent nanocrystalline yttria stabilized zirconia. *Opt Mater* 2009; 32: 62–68.

7. Plashnitsa VV, Elumalai P, Fujio Y, et al. Zirconia-based electrochemical gas sensors using nano-structured sensing materials aiming at detection of automotive exhausts. *Electrochim Acta* 2009; 54: 6099–6106.
8. Park S, Vohs JM and Gorte RJ. Direct oxidation of hydrocarbons in a solid-oxide fuel cell. *Nature* 2000; 404: 265–267.
9. Baeza P, Aguila G, Vargas G, et al. Adsorption of thiophene and dibenzothiophene on highly dispersed Cu/ZrO₂ adsorbents. *Appl Catal B Environ* 2012; 111–112: 133–140.
10. Espinoza-González R, Mosquera E, Moglia Í, et al. Hydrothermal growth and characterization of zirconia nanostructures on non-stoichiometric zirconium oxide. *Ceram Int* 2014; 40: 15577–15584.
11. Podsiadlo P, Kaushik AK, Arruda EM, et al. Ultrastrong and stiff layered polymer nanocomposites. *Science* 2007; 318: 80–83.
12. Huang ZH and Oiu KY. Preparation and thermal property of poly(methyl methacrylate)/silicate hybrid materials by the in-situ sol-gel process. *Polym Bull* 1995; 35: 607–613.
13. Wang HT, Xu P, Zhong W, et al. Transparent poly(methyl methacrylate)/silica/zirconia nanocomposites with excellent thermal stabilities. *Polym Degrad. Stabil* 2005; 87: 319–327.
14. Lazouzi G, Vuksanović MM, Tomić NZ, et al. Optimized preparation of alumina based fillers for tuning composite properties. *Ceram Int* 2018; 44: 7442–7449.
15. Elmadani AA, Tomić N, Petrović M, et al. Influence of surface modification to mechanical and thermal properties of nanomodified acrylic dental resin. *Dig J Nanomater Bios* 2018; 13: 23–29.
16. Algellai AA, Vuksanović MM, Tomić NZ, et al. Improvement of cavitation resistance of composite films using functionalized alumina particles. *Hem Ind* 2018; 72: 205–213.
17. Kovačević T, Rusmirović J, Tomić N, et al. New composites based on waste PET and non-metallic fraction from waste printed circuit boards: mechanical and thermal properties. *Compos Part B Eng* 2017; 127: 1–14.
18. ASTM E384 - 16, ASTM E384 - 16 - Stand. Test Method Microindentation Hardness Mater. 201528. (n.d.).
19. Iost A and Bigot R. Hardness of coatings. *Surf Coatings Technol* 1996; 80: 117–120.
20. Ahmed Ben Hasan S, Dimitrijević MM, Kojović A, et al. The effect of alumina nanofillers size and shape on mechanical behavior of PMMA matrix composite. *J Serb Chem Soc* 2014; 79: 1–19.
21. Alzarrug FA, Dimitrijević MM, Jančić Heinemann RM, et al. The use of different alumina fillers for improvement of the mechanical properties of hybrid PMMA composites. *Mater Design* 2015; 86: 575–581.
22. Lazouzi GA, Vuksanović MM, Tomić N, et al. Dimethyl itaconate modified PMMA - alumina fillers composites with improved mechanical properties. *Polym Composites* 2019; 40: 1691–1701.
23. Kraus W and Nolze G. *Powdercell for windows*. Vol. 2.4. Berlin: Federal Institute for Materials Research and Testing, 2000.
24. Vitanov P, Harizanova A and Ivanova T. Characterization of ZrO₂ and (ZrO₂)_x(Al₂O₃)_{1-x} thin films on Si substrates: effect of the Al₂O₃ component. *J Phys Conf Ser* 2014; 514: 012011.
25. Guo GY and Chen YL. Unusual structural phase transition in nanocrystalline zirconia. *Appl Phys A* 2006; 84: 431–437.
26. Socrates G. *Infrared and Raman characteristic group frequencies. tables and charts*. Hoboken: John Wiley, 2001.
27. Boumaza A, Favaro L, Ledion J, et al. Transition alumina phases induced by heat treatment of boehmite: An X-ray diffraction and infrared spectroscopy study. *J Solid State Chem* 2009; 182: 1171–1176.
28. Zhang Y, Xi H., Chen L, et al. A comparison study of the structural and mechanical properties of cubic, tetragonal, monoclinic, and three orthorhombic phases of ZrO₂. *J Alloy Compd* 2018; 749: 283–292.
29. Wanga G, Menga F, Dinga C, et al. Microstructure, bioactivity and osteoblast behavior of monoclinic zirconia coating with nanostructured surface. *Acta Biomater* 2010; 6: 990–1000.
30. Bernard O, Huntz AM, Andrieux M, et al. Synthesis, Structure, microstructure and mechanical characteristics of MOCVD deposited zirconia films. *Appl Surf Sci* 2007; 253: 4626–4640.
31. Corrêa de Sá e Benevides de Moraes MC, Elias CN, Filhob JD, et al. Mechanical properties of alumina-zirconia composites for ceramic abutments. *Mater Res Ibero Am J* 2004; 7: 643–649.